Available online at www.sciencedirect.com
SCIENCE DIRECT®
Composites Science and Technology 63 (2003) 2379–2387
COMPOSITES SCIENCE AND TECHNOLOGY
www.elsevier.com/locate/compscitech

Synthesis of porous cross-linked polymer monoliths using 1,1,1,2-tetrafluoroethane (R134a) as the porogen

Andrew K. Hebb, Kazunobu Senoo, Andrew I. Cooper*

Donnan and Robert Robinson Laboratories, Department of Chemistry, University of Liverpool, Crown Street, Liverpool L69 3BX,UK

Abstract

In this paper, we describe the synthesis of porous, cross-linked polymethacrylate monoliths by free radical polymerization using 1,1,1,2-tetrafluoroethane (R134a) as the porogenic solvent. Solvent separations were simple (boiling point R134a = −26.5 °C) and the reactions were carried out at relatively low pressures (<20 bar). It was found that the surface area and the median pore diameter of the materials could be varied over a wide range (5–320 m^2/g and 15 nm–5 μm, respectively) by varying the monomer concentration. By contrast, pressure had little influence on the structure of the materials due to the relatively incompressible nature of liquid R134a.

1. Introduction

Highly cross-linked, permanently porous polymers are useful in a wide range of applications [1,2]. Unlike lightly cross-linked gel-type polymers which become porous when swollen by solvents, more highly cross-linked polymers have a permanent porous structure which is formed during their preparation and persists in the dry state [2]. The internal porous morphology is characterized by interconnected channels (pores) which permeate the rigid, extensively cross-linked polymer matrix. In the literature on porous resins, the term macroporous is often used to refer to materials with permanent porosity in the dry state, irrespective of pore size. To avoid confusion, we have restricted our use of the terms micropore, mesopore, and macropore to the definitions recommended by IUPAC [3] i.e., micropores <2 nm, mesopores 2–50 nm, macropores >50 nm. When referring to porous structures in general, we have adopted the expression permanently porous, as proposed by Rohr et al. [4].

Permanently porous materials are often synthesized in the form of uniform beads by suspension polymerization [4–8]. This leads to performance limitations in certain applications, notably the chromatographic separation of large molecules. The passage of molecules within the pores is typically controlled by diffusion. Diffusion constants for large molecules, such as proteins or synthetic polymers, are several orders of magnitude lower than for small molecules, causing problems in applications such as chromatography where the separation efficiency is strongly dependent on mass transfer rates. Modern HPLC methods frequently involve columns packed with porous polymer beads [9–11]. The flow of the mobile phase between the beads through the large interstitial voids in the column is relatively unimpeded, whereas liquid present in the network of resin pores does not flow and remains stagnant. For large molecules, diffusional mass transfer rates between the interstitial voids and the pores may be very slow, thus causing peak broadening and necessitating low flow rates or longer columns. A promising approach to this problem has been the synthesis of continuous, porous monolithic polymers [12,13] which have been developed for a variety of applications including HPLC [14], high-performance membrane chromatography (HPMC) [15], capillary electrochromatography [16–19], microfluidics [20,21], molecular imprinting [22], and high-throughput bioreactors [23]. Typically, a mold is filled with a polymerization mixture containing a cross-linking monomer, functional comonomer(s), initiator, and a porogenic diluent. This mixture is then polymerized, either thermally or photochemically, to form a continuous porous monolith which conforms to the shape of the mold. Many systems have involved the free radical polymerization of methacrylate or styrene based

* Corresponding author. Tel.: +44-151-7943548; fax: +44-151-7943588.
E-mail address: aicooper@liverpool.ac.uk (A.I. Cooper).

0266-3538/$ - see front matter © 2003 Elsevier Ltd. All rights reserved.
doi:10.1016/S0266-3538(03)00271-9

cross-linkers, e.g., ethylene glycol dimethacrylate (EGDMA), divinyl benzene (DVB). The porogenic diluent may be either solvating or non-solvating in nature, and carefully chosen ternary solvent mixtures can be used to allow fine control of the porous properties of the monolithic polymers [16–18,24]. In some cases, materials have been optimized to incorporate a distribution of small, diffusive pores (<100 nm), interconnected with larger, flow-through pores with diameters in the range 700–2000 nm [25]. The large pores provide permeability through the monolith and also facilitate convection, thus greatly enhancing mass transport. A key advantage of this methodology is that the porous polymers can be prepared directly within a variety of different containment vessels, including wide bore chromatography columns, narrow bore capillaries, and microfluidic devices. There are also disadvantages associated with the monolith approach: for example, the synthesis is solvent intensive and it may be difficult to remove solvent residues from the continuous materials after polymerization. Furthermore, highly cross-linked, permanently porous polyacrylates are quite often brittle and easily damaged, thus necessitating suitable permanent containment to allow handling (e.g., in capillaries or columns).

Previously, we have described the synthesis of highly cross-linked porous polymer monoliths [26,27] and beads [28] using supercritical carbon dioxide ($scCO_2$) as the porogenic diluent. Carbon dioxide is an attractive solvent for polymer chemistry because it is inexpensive, non-toxic, and non-flammable [29–31]. Unlike conventional liquid solvents, supercritical fluids (SCFs) are highly compressible and the density (and therefore solvent properties) can be tuned over a wide range by varying pressure [32]. Moreover, SCFs revert to the gaseous state upon depressurization, simplifying the separation of solvent from solute and eliminating solvent residues. In addition to the synthesis of porous cross-linked vinyl polymers, $scCO_2$ has been used for the formation of aerogels [33], microcellular polymer foams [34–36], porous biopolymer composites [37], and emulsion-templated polyHIPE materials [38].

We have shown that permanently porous polymer can be formed in $scCO_2$ by the polymerization of cross-linking monomers such as EGDMA and trimethylolpropane trimethacrylate (TRIM). At relatively low monomer concentrations (<30% w/v), non- porous microgel powders were observed [39,40]. At higher monomer concentrations (40–60% v/v), continuous porous polymer monoliths were produced [26,27]. These materials conformed to the shape of the reaction vessel (i.e., they were molded). For polymers formed from TRIM, an increase in monomer concentration led to a marked decrease in the median pore size and a corresponding increase in the specific surface area. It was found that relatively small changes in the monomer concentration could lead to dramatic changes in the resulting polymer structure. We showed that polymer properties such as pore size, pore volume, and surface area all showed a strong dependence on the CO_2 pressure [41]. As such, the reaction pressure can be used to fine tune the pore structure in these materials, thus exploiting the compressible nature of these SCF solvents in a practically useful way [28,41].

By contrast, a disadvantage associated with the use of $scCO_2$ for polymerization is that relatively high reaction pressures (800–5000 psi) may be required, particularly in applications that operate well above the critical temperature ($T_c = 31.1$ °C) and that require liquid-like solvent densities (>0.7 g/cm^3). In the short term, high pressures translate into increased capital equipment costs. In the longer term, large pressure differentials contribute to operating costs and to overall energy consumption [42]. We have commenced a series of studies to evaluate hydrofluorocarbon (HFC) liquids, such as 1,1,1,2-tetrafluoroethane (R134a), as potential solvents for polymerization. Like CO_2, R134a is non-flammable and has zero ozone depletion potential. Assessment of the global warming potential (GWP) for R134a (and other HFCs) requires a detailed knowledge of both the atmospheric lifetime and the infrared absorption cross-section in the atmospheric transparency window (8–12 μm). Although the precise GWP for 7 HFCs is still the subject of debate, a widely held view is that the impact of these CFC-replacements on climate change will be a very small fraction of the total impact, which will come mainly from the accumulation of CO_2 in the atmosphere [43]. Thus, R134a has found widespread use in refrigeration and in auto air conditioning systems. In addition, the low toxicity of R134a has led to FDA approval as a propellant in metered dose inhalers [44]. In principle, the low pressures required to liquefy R134a could equate to reduced operating costs. On the other hand, HFCs are much more expensive than CO_2,[1] and efficient recycling of these fluids would certainly be a prerequisite for industrial-scale use. Energy-efficient solvent recycling may be practical for R134a since the fluid was originally developed as a refrigerant. Previously, HFC solvents have been evaluated in applications such as electrochemistry [45,46], particle formation [47,48], extraction [49], and polymer foaming [50].

We have found that R134a ($T_c = 101.1$ °C, $P_c = 40.6$ bar) can be used as a solvent for dispersion polymerization at much lower pressures than are feasible with $scCO_2$ [51,52]. We have also shown that it is possible to carry out dispersion polymerization in R134a using inexpensive hydrocarbon stabilizers, as opposed to the

[1] Current price for refrigeration grade R134a is approximately $2 per pound.

relatively expensive fluorinated materials used in conjunction with CO_2-based processes [29,30].

In this paper, we demonstrate that R134a may be used as a porogenic solvent for the synthesis of porous cross-linked polymethacrylate monoliths. Solvent separation is simple because the solvent reverts to the gaseous state upon depressurization (b.p. R134a = −26.5 °C). Moreover, these reactions may be conducted at much lower pressures (< 20 bar) than are possible with $scCO_2$.

2. Experimental section

2.1. Materials

Trimethylolpropane trimethacrylate (TRIM, Aldrich) was used as received. 2,2-Azobisisobutyronitrile (AIBN) was recrystallized twice from methanol and dried under vacuum before use. 1,1,1,2-Tetrafluoroethane (R134a, refrigeration grade) was purchased from Ineos Fluor (Runcorn, UK) and was passed over an Oxisorb catalyst (Messer Griesheim) in order to remove any traces of oxygen.

2.2. Equipment

R134a was added to the reaction vessel using an Isco 260D syringe pump. The pressure in the reactor was measured with a pressure transducer (A105, RDP Electronics) and a digital display (E308, RDP Electronics). The internal reactor temperature was measured with an industrial mineral isolated thermocouple (Type K, RS Electronics). A PTFE-coated magnetic stir bar was used to mix the contents of the reactor before polymerization. The reactor was placed on its side such that the long axis was horizontal.

2.3. Polymerization

Reactions were carried out in a 10 cm^3 stainless-steel view cell, as described previously [40]. Briefly, the monomer and the initiator were added to the reactor which was then purged with a slow stream of R134a for 10 min to remove any oxygen. A measured volume of liquid R134a was then added to the reaction vessel and the mixture stirred at room temperature until a single homogeneous phase was observed. The reactor was then heated to 60 °C (±0.5 °C) in order to initiate the polymerization. Phase behavior was observed through the sapphire window in the reaction vessel. The R134a was removed at the end of the reaction by depressurization. The rate of pressure release had no obvious influence on the polymer morphology since the materials were highly cross-linked and not subject to expansion or foaming [34–37]. No cracks were observed to form in the monolithic materials, even when the pressure was released quite rapidly. Monomer conversions were 95–100% in all cases.

2.4. Characterization

For analysis, the continuous polymer samples were fractured into millimeter-sized pieces with a scalpel. Pore size distributions were recorded by mercury intrusion porosimetry using a Micromeritics Autopore IV 9500 porosimeter. Samples were subjected to a pressure cycle starting at approximately 0.5 psia, increasing to 60,000 psia in predefined steps to give pore size /pore volume information. Polymer surface areas were measured using the BET method with a Micromeritics ASAP 2010 nitrogen adsorption analyzer. Samples were outgassed for 3 h at 60 °C under N_2 flow before analysis. BET surface areas, pore volumes, and micropore surface areas (BJH) were calculated using the Micromeritics software package (version 5.0). Absolute densities were measured using a Micromeritics Helium AccuPyc 1330 pycnometer. Polymer morphologies were investigated with a Hitachi S-2460N scanning electron microscope (SEM). Samples were mounted on aluminium studs using adhesive graphite tape and sputter coated with approximately 10 nm of gold before analysis.

3. Results and discussion

From the viewpoint of a synthetic polymer chemist, the solvent properties of R134a are somewhat similar to those of $scCO_2$. For example, we have found that the majority of common vinyl monomers are soluble (at least up to 20–50%v/v) in liquid R134a at room temperature and above [51,52]. Similarly, most hydrocarbon polymers that we have investigated so far (with the exception of polyvinylacetate) [52] exhibit very low solubility in liquid R134a under moderate conditions (T < 100 °C, P < 50 bar) when the molecular weight is higher than a few thousand mass units. An important difference between R134a and CO_2 is solvent polarity: CO_2 is symmetrical and has no dipole moment, while R134a is moderately polar and has a significant dipole moment (2.1 D) [53]. The critical temperature for R134a is 101.1 °C: thus, it is possible to carry out reactions in the *liquid* state at quite moderate pressures (5–50 bar) at temperatures between ambient and 100 °C. Moreover, the solvent density under these conditions (for pure R134a) ranges between 0.9 and 1.3 g/cm^3 [54]. This is significant because many polymerization reactions proceed at temperatures that are well above ambient. Liquid CO_2 can be used as a solvent at relatively low pressures (< 70 bar), but only for reactions occurring at temperatures below 31.1 °C. In the case of the free-radical polymerization, this requires the use of low-temperature initiators that may be difficult to transport

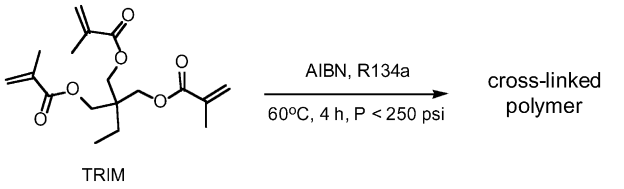

Fig. 1. Preparation of cross-linked polyTRIM monoliths using R134a as the porogenic solvent.

and handle. All of the reactions described here were carried out using a common free radical initiator at a temperature (60 °C) where R134a exists in the liquid state.

3.1. Effect of monomer concentration

A series of experiments was conducted in which we synthesized polyTRIM monoliths (Fig. 1) over a range of monomer concentrations with respect to the solvent (i.e., the porogen), as summarized in Table 1. Apart from the ratio of monomer (TRIM) to solvent (R134a), all other variables (i.e., reactor volume, initiator concentration, heating rate, reaction temperature) were kept constant. Fig. 2 shows the effect of the monomer to solvent ratio on the BET surface area for these materials. Low monomer concentrations (<0.4 g/cm^3) were not sufficient to form continuous monoliths materials, and the polymers were isolated as loosely agglomerated microgel powders, as noted previously for the precipitation polymerisation of cross-linking monomers such as DVB, EGDMA, and TRIM in $scCO_2$ [39,40]. These materials exhibited low BET surface areas (<20 m^2/g, Fig. 2). At higher monomer concentrations (0.5–1.2 g/cm^3), a sharp increase in the BET surface area was observed (Fig. 2) and the materials were isolated as continuous, porous monoliths that conformed to the shape of the reaction vessel. A maximum in the BET surface area of ~320 m^2/g was observed at monomer concentrations of around 1.2 g/cm^3 TRIM. In this concentration range, the materials varied in nature from soft, crumbly materials (0.6 g/cm^3 TRIM) to harder, brittle monoliths (1.2 g/cm^3 TRIM). All of the materials

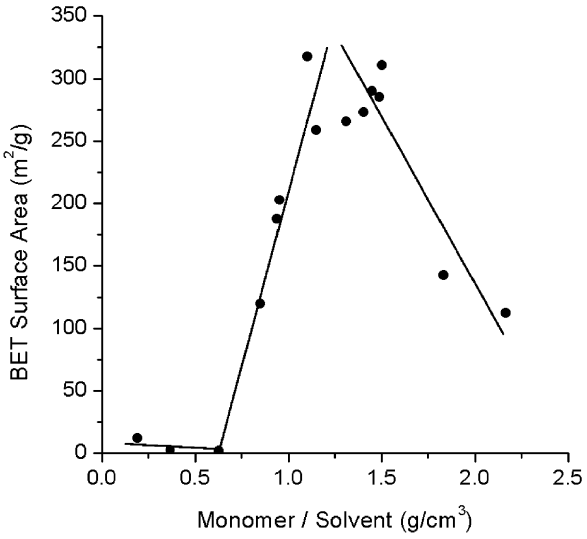

Fig. 2. Variation in BET surface area for polyTRIM monoliths synthesized over a range of TRIM concentrations using R134a as the porogenic solvent.

Table 1
Effect of monomer to porogen ratio on physical properties of macroporous crosslinked TRIM monoliths synthesized using R134a as the porogenic solvent[a]

	Monomer/R134a (g/cm^3)[b]	Final pressure (psi)[c]	Surface area (m^2/g)[d]	Absolute density (g/cm^3)[e]	Median pore diameter (nm)[f]	Intrusion volume (cm^3/g)[e]
1	0.190	250	12	1.345	4090	4.307
2	0.364	252	3	1.254	5396	3.483
3	0.626	251	2	1.220	3964	1.144
4	0.849	244	120	1.227	135	1.219
5	0.936	230	188	1.253	47.9	0.944
6	0.950	236	203	1.230	51.5	1.000
7	1.100	237	318	1.283	45.6	0.833
8	1.145	231	259	1.242	32.8	0.646
9	1.311	249	266	1.217	35.0	0.640
10	1.403	233	273	1.240	33.1	0.463
11	1.446	230	290	1.236	22.1	0.290
12	1.486	216	285	1.222	31.4	0.532
13	1.502	218	311	1.213	31.4	0.264
14	1.831	204	143	1.219	12.8	0.226
15	2.163	200	113	1.213	15.7	0.181

[a] Reaction conditions: AIBN (2%w/w based on TRIM), 60 °C, 4 h.
[b] Mass of TRIM monomer divided by volume of R134a added.
[c] Pressure recorded at 60 °C after reaction in complete.
[d] Measured by N_2 adsorption-desorption using the Brunauer–Emmett–Teller method
[e] Measured by helium pycnometry
[f] Measured by mercury intrusion porosimetry over the pore size range 7 nm°–100 μm.

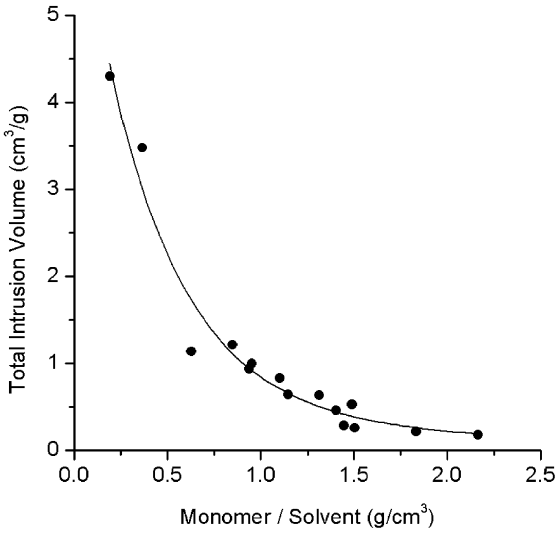

Fig. 3. Variation in total intrusion volume (pore volume) for polyTRIM monoliths synthesized over a range of TRIM concentrations using R134a as the porogenic solvent (measured by mercury intrusion porosimetry over the pore diameter range 7 nm–100 μm).

were opaque white in appearance. At higher TRIM concentrations (1.2–2.2 g/cm^3), the BET surface area fell sharply (~100 m^2/g at ~2.2 g/cm^3 TRIM, Fig. 2). At these higher monomer concentrations, the materials were isolated as denser, semi-transparent, brittle monoliths. The variation in the total intrusion volume (i.e., the pore volume, as measured by mercury intrusion porosimetry over the range 7 nm–100 μm), is shown in Fig. 3. It was found that the intrusion volume fell exponentially as a function of the monomer to solvent ratio. Similarly, the median pore diameter, as measured by mercury intrusion porosimetry, was also found to fall very sharply as the monomer concentration was increased (Fig. 4). (It should be noted that the pore size distributions in these samples are often broad: as such, the changes in the median pore diameter measured by mercury intrusion porosimetry reflect general shifts in the position of the pore distribution envelope, rather than the position of a well-defined, sharp peak.) The monomer concentration has almost no effect on the absolute density of these materials, as measured by helium pycnometry (Fig. 5).

All of these effects are consistent with studies involving more conventional organic solvents as porogens [16–18,24,25]. At low monomer concentrations ([TRIM] < 0.4 g/cm^3), monolithic polymers are not formed and the products are isolated as microgel powders. These powders have a relatively coarse structure (see Fig. 6a) and hence exhibit low surface areas. As the monomer concentration is increased ([TRIM] = 0.5–1.2 g/cm^3), monolithic polymers are observed that conform to the interior of the reaction vessel. These materials exhibit much finer internal structures (i.e., the fused polymer particles that make up the material are much less coarse, see Figs. 6b and 6c). Consequently, there is a sharp increase in the surface area of these materials over this concentration range because the average pore size (i.e., the width of the spaces between the fused particles) decreases dramatically (Fig. 4). This sharp decrease in the median pore diameter outweighs the decrease in the total pore volume (Fig 3) observed as the monomer concentration is increased over this range (i.e., even though the pore volume decreases significantly, the pore size decreases much more dramatically and hence surface area increases). As the monomer concentration is increased over the range 1.2–2.2 g/cm^3, the reverse trend

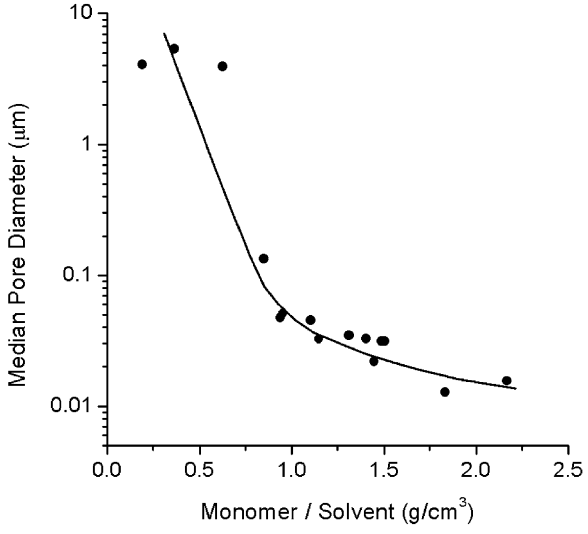

Fig. 4. Variation in median pore diameter for polyTRIM monoliths synthesized over a range of TRIM concentrations using R134a as the porogenic solvent (measured by mercury intrusion porosimetry over the pore diameter range 7 nm–100 μm).

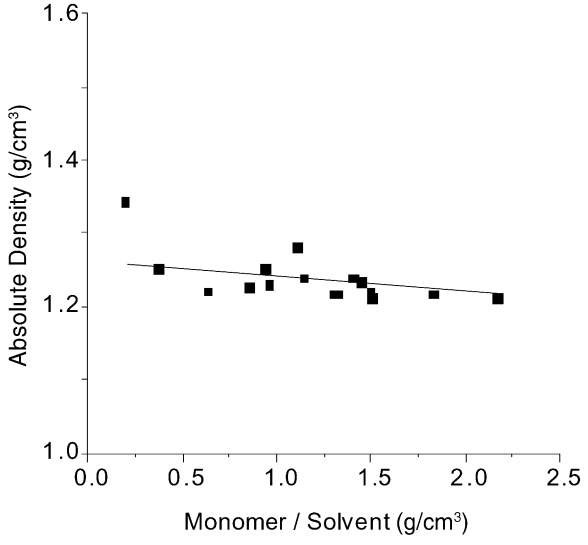

Fig. 5. Variation in absolute density for polyTRIM monoliths synthesized over a range of TRIM concentrations using R134a as the porogenic solvent (measured by helium pycnometry).

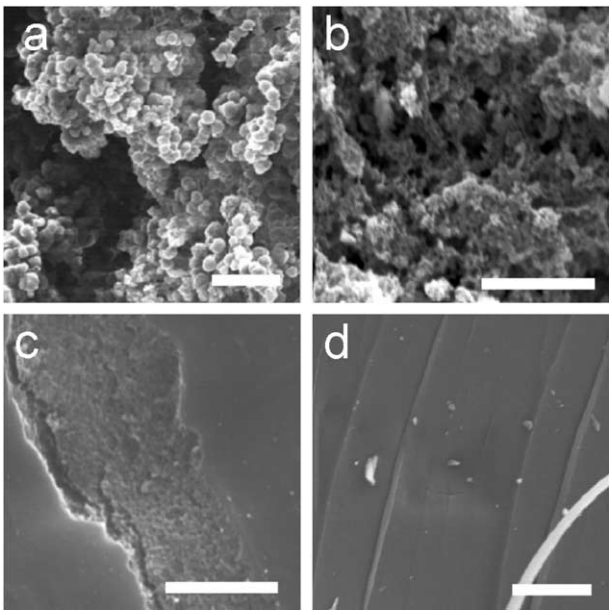

Fig. 6. Electron micrographs for polyTRIM monoliths synthesized using R134a as the porogenic solvent at different TRIM concentrations (scale bar = 10 μm in all images): (a) sample 1,surface area = 12 m^2/g; (b) sample 6, surface area = 203 m^2/g; (c) sample 7,surface area = 318 m^2/g; (d)sample 15,surface area = 113 m^2/g.

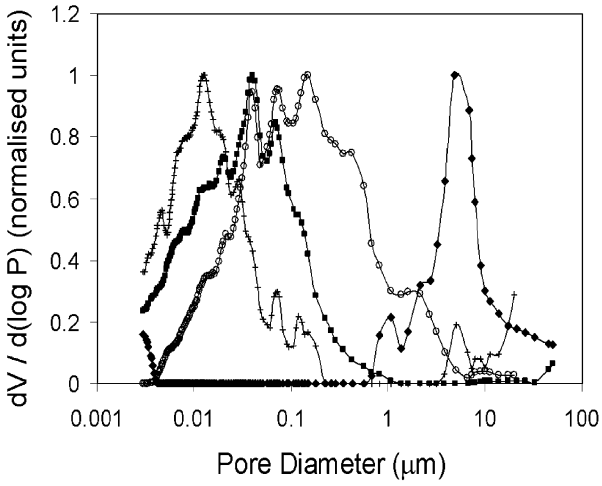

Fig. 7. Pore size distributions for polyTRIM monoliths synthesized using R134a as the porogenic solvent at different TRIM concentrations (measured by mercury intrusion porosimetry over the pore diameter range 7 nm–100 μm); Filled diamond points: sample 2, median pore diameter = 5.4 μm; Open circle points: sample 4, median pore diameter = 47.9 nm; Filled square points: sample 7, median pore diameter = 45.6 nm; Cross points: sample 15, median pore diameter = 15.7 nm.

is observed: the decrease in pore diameter is relatively small (Fig. 4) and the decrease in the total pore volume (Fig. 3) dominates,[2] such that a reduction in surface area is observed.

It is clear that the pore volume should fall as the ratio of monomer to porogen is increased. By contrast, the factors that affect the polymer structure and the average pore size are more subtle [2,16–18,24–27]. We rationalize the observed variations by considering the mechanism of formation of the polymeric matrix. R134a is a very poor solvent for most polymers, and is certainly a non-solvent for PMMA (i.e., the linear equivalent of polyTRIM) [51,52]. The monomer (TRIM) can be considered as a much better thermodynamic solvent for the growing polymer matrix than R134a. Thus, at low TRIM concentrations, phase separation would be expected to occur at rather lower polymer conversions. Fused microgel particles are formed, a significant quantity of polymer is generated *after* phase separation, both in the monomer-swollen microgel particles and in the R134a-rich phase. This leads to growth of the fused particles and to in-filling of small pores between the particles, thus forming larger, fused aggregates with relatively low surface areas (Figs 6a,b). By contrast, polymer network phase separation might be expected to occur somewhat later in reactions involving higher monomer concentrations, since TRIM is the better solvent for the polymer network. When phase separation does occur, the microgel particles are therefore relatively small and discrete, and are fused together by further polymerization in the R134a-rich phase, giving rise to smaller pores (Fig. 6c,d).

Fig. 7 shows the pore size distributions, as measured by mercury intrusion porosimetry, for four polyTRIM materials synthesized at increasing TRIM concentrations. The median pore diameter can be shifted over a very wide range (10 nm–10 μm) in this system. Some materials (e.g., sample 4) exhibit broad pore size distributions that encompass larger pores (100 nm-10 mm) interconnected with small pores (< 50 nm). Materials such as this may be very useful for flow-through applications since the large pores facilitate flow whilst the small pores provide surface area (BET surface area for sample 4 = 120 m^2/g).

3.2. Effect of reaction pressure

Previously, we showed that pressure has a strong effect on polymer properties such as pore size, pore volume, and surface area for cross-linked polymers produced in $scCO_2$ [41]. In the system presented here, the porogen is used in the liquid state; as such, the compressibility is much lower and one might expect the effect of pressure to be much less marked for fluids used in the liquid state. This was indeed found to be the case. Table 2 lists the properties for a series of polyTRIM materials synthesized at a fixed monomer concentration but at varying R134a-pressures (i.e., the reactor was filled and slightly overpressurized above the liquid vapour

[2] Note that mercury intrusion porosimetry only measures pores with diameters > 7 nm.

Table 2
Effect of R134a pressure on physical properties of macroporous crosslinked TRIM monoliths[a]

	Final pressure (Kpsi)[b]	Surface area (m^2/g)[c]	Micropore surface area (m^2/g)[d]	Micropore surface area (%)[c]	Absolute density (g/cm^3)[d]	Median pore diameter (nm)[e]	Intrusion volume (cm^3/g)[e]
16	0.237	281	28	10.1	1.230	42.5	0.445
17	0.260	298	64	21.4	1.230	34.1	0.718
18	0.266	390	80	20.6	1.225	46.8	0.604
19	0.293	355	62	17.5	1.234	39.9	0.766
20	0.376	345	61	17.5	1.238	38.5	0.670
21	0.387	351	60	17.2	1.216	31.5	0.700
22	0.465	321	50	15.6	1.231	42.0	0.929

[a] Reaction conditions: TRIM (5.5 cm^3, 6.06 g), AIBN (2% w/w based on TRIM), 60 °C, 4 h.
[b] Pressure recorded at 60 °C after reaction in complete.
[c] Measured by N_2 adsorption-desorption using the Brunauer–Emmett–Teller method.
[d] Measured by helium pyknometry.
[e] Measured by mercury intrusion porosimetry over the pore size range 7 nm–100 μm.

pressure of R134a). A degree of variation was observed in the surface area of the materials (Fig. 8), but the dependence of pressure was relatively small. The median pore diameter (Fig. 9) did not vary at all as a function of R134a pressure, quite unlike the equivalent system involving $scCO_2$, where a strong pressure-dependence was found [41]. Both of these observations are consistent with the fact that the solvent quality of the porogen that affects the process of phase separation in these materials. Solvent quality varies dramatically with pressure in the case of SCFs, whereas for relatively incompressible liquid solvents, it does not [32].

3.3. In situ synthesis of porous chromatography packings

We have shown that this technique can be used to prepare porous monolithic polymer materials directly within common stainless steel chromatography columns. Fig. 10 shows a photograph of such a material. This particular packing was produced using $scCO_2$ as the porogen, although R134a can be used in a similar way. Under the appropriate conditions (particularly with respect to monomer concentration), it is possible to prepare these materials without significant shrinkage, thus forming a porous packing that fills the entire column. Again, no organic solvents are used in this process, and it is possible to remove any monomer residues by in situ supercritical fluid extraction at the end of the polymerization. Control over pore volume and pore size distribution is vital in the production of chromatographic stationary phases, and we believe that our approach has the potential to allow fine tuning of these parameters as well as greatly reducing the volume of organic solvent used in the process.

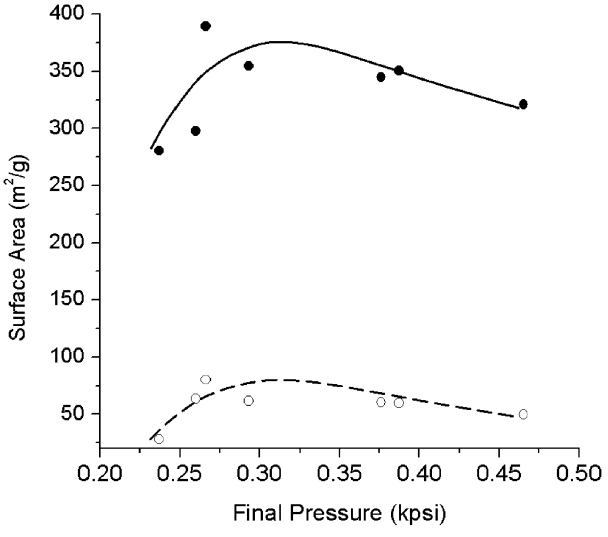

Fig. 8. Variation in BET surface area for polyTRIM monoliths synthesized at various R134a pressures.

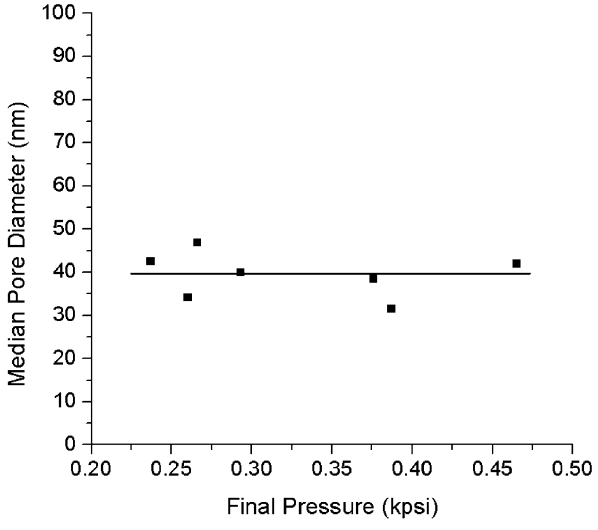

Fig. 9. Variation in median pore diameter for polyTRIM monoliths synthesized at various R134a pressures (measured by mercury intrusion porosimetry over the pore diameter range 7 nm–100 μm).

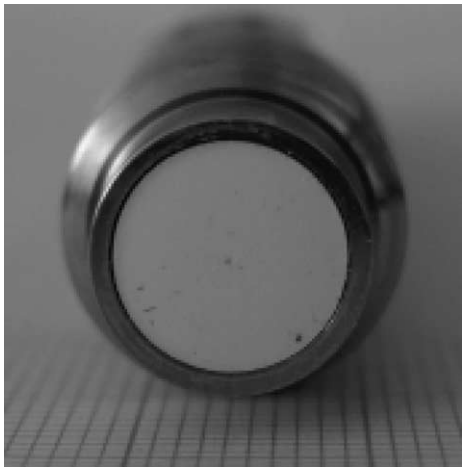

Fig. 10. Porous polyTRIM monolith synthesized in a 10 mm diameter stainless steel column using $scCO_2$ as the porogen (column volume = 8 cm^3; TRIM volume = 4 cm^3; P = 4000 psi; 2%w/v AIBN). Note that the porous polyTRIM material fills the entire column without significant shrinkage, either during polymerization or during depressurization.

4. Conclusions

In this paper, we show that R134a can be used as a porogenic solvent for the preparation of cross-linked polymethacrylate monoliths. Due to the low boiling point of the porogen (−26.5 °C), solvent separation is simple and no washing or drying steps are required. Moreover, since R134a is non-toxic, this approach may offer a potential route to solvent-free biocomposites. The polymer synthesis is carried out at much lower pressures than are possible with $scCO_2$ (i.e., 15–20 bar compared to 150–300 bar). Average pore sizes and surface areas in the materials may be varied over a wide range by varying the monomer concentration. By contrast, pressure has rather little effect due to the relatively incompressible nature of liquid R134a. Future studies will focus on the applications of materials produced by this route.

Acknowledgements

We thank EPSRC for funding (GR/23653 + GR/R15597). AIC acknowledges the support of the Royal Society through the provision of a Research Fellowship.

References

[1] Hodge P, Sherrington DC. Syntheses and separations using functional polymers. New York: Wiley; 1989.
[2] Sherrington DC. Preparation, structure and morphology of polymer supports. Chem Commun 1998:2275–86.
[3] Sing KSW, Everett DH, Haul RAW, Moscou L, Pierotti RA, Rouquerol J, et al. Reporting physisorption data for gas solid systems with special reference to the determination of surface-area and porosity (Recommendations 1984). Pure Appl Chem 1985;57:603–19.
[4] Rohr T, Knaus S, Gruber H, Sherrington DC. Preparation and porosity characterization of highly cross-linked polymer resins derived from multifunctional (meth)acrylate monomers. Macromolecules 2002;35:97–105.
[5] Yuan HG, Kalfas G, Ray WH. Suspension polymerization. J Macromol Sci, Rev Macromol Chem Phys 1991;C31:215–99.
[6] Arshady R. Suspension, emulsion, and dispersion polymerisation—a methodological survey. Colloid Polym Sci 1992;270:717–32.
[7] Vivaldo-Lima E, Wood PE, Hamielec AE, Penlidis A. An updated review on suspension polymerization. Ind Eng Chem Res 1997;36:939–69.
[8] Lewandowski K, Svec F, Fr chet JMJ. Polar, monodisperse, reactive beads from functionalized methacrylate monomers by staged templated suspension polymerization. Chem Mater 1998; 10:385–91.
[9] Lewandowski K, Murer P, Svec F, Fréchet JMJ. Highly selective chiral recognition on polymer supports: preparation of a combinatorial library of dihydropyrimidines and its screening for novel chiral HPLC ligands. Chem Commun 1998;18:2237–8.
[10] Murer P, Lewandowski K, Svec F, Fréchet JMJ. On-bead combinatorial approach to the design of chiral stationary phases for HPLC. Anal Chem 1999;71:1278–84.
[11] Xu MC, Brahmachary E, Janco M, Ling FH, Svec F, Fréchet JMJ. Preparation of highly selective stationary phases for high-performance liquid chromatographic separation of enantiomers by direct copolymerization of monomers with single or twin chiral ligands. J Chromatogr A 2001;928:25–40.
[12] Svec F, Fréchet JMJ. New designs of macroporous polymers and supports: From separation to biocatalysis. Science 1996;273:205–11.
[13] Peters EC, Svec F, Fréchet JMJ. Rigid macroporous polymer monoliths. Adv Mater 1999;11:1169–81.
[14] Xie S, Svec F, Fréchet JMJ. Rigid porous polyacrylamide-based monolithic columns containing butyl methacrylate as a separation medium for the rapid hydrophobic interaction chromatography of proteins. J Chromatogr A 1997;775:65–72.
[15] Tennikov MB, Gazdina NV, Tennikova TB, Svec F. Effect of porous structure of macroporous polymer supports on resolution in high-performance membrane chromatography of proteins. J Chromatogr A 1998;798:55–64.
[16] Peters EC, Petro M, Svec F, Fréchet JMJ. Molded rigid polymer monoliths as separation media for capillary electrochromatography. Anal Chem 1997;69:3646–9.
[17] Peters EC, Petro M, Svec F, Fréchet JMJ. Molded rigid polymer monoliths as separation media for capillary electrochromatography 1. Fine control of porous properties and surface chemistry. Anal Chem 1998;70:2288–95.
[18] Peters EC, Petro M, Svec F, Fréchet JMJ. Molded rigid polymer monoliths as separation media for capillary electrochromatography 2. Effect of chromatographic conditions on the separation. Anal Chem 1998;70:2296–302.
[19] Schweitz L, Andersson LI, Nilsson S. Capillary electrochromatography with predetermined selectivity obtained through molecular imprinting. Anal Chem 1997;69:1179–83.
[20] Rohr T, Yu C, Davey MH, Svec F, Fréchet JMJ. Porous polymer monoliths: Simple and efficient mixers prepared by direct polymerization in the channels of microfluidic chips. Electrophoresis 2001;22:3959–67.
[21] Yu C, Xu MC, Svec F, Fréchet JMJ. Preparation of monolithic polymers with controlled porous properties for microfluidic chip applications using photoinitiated free-radical polymerization. J Polym Sci A, Polym Chem 2002;40:755–69.
[22] Whitcombe MJ, Vulfson EN. Imprinted polymers. Adv Mater 2001;13:467–78.

[23] Petro M, Svec F, Fréchet JMJ. Immobilization of trypsin onto "molded" macroporous poly(glycidyl methacrylate-co-ethylene dimethacrylate) rods and use of the conjugates as bioreactors and for affinity chromatography. Biotech Bioeng 1996;49:355–63.
[24] Santora BP, Gagne MR, Moloy KG, Radu NS. Porogen and cross-linking effects on the surface area, pore volume distribution, and morphology of macroporous polymers obtained by bulk polymerization. Macromolecules 2001;34:658–61.
[25] Svec F, Fréchet JMJ. Kinetic control of pore formation in macroporous polymersFormation of "molded" porous materials with high flow characteristics for separations or catalysis. Chem Mater 1995;7:707–15.
[26] Cooper AI, Wood CD, Holmes AB. Synthesis of well-defined macroporous polymer monoliths by sol-gel polymerization in supercritical CO_2. Ind Eng Chem Res 2000;39:4741–4.
[27] Cooper AI, Holmes AB. Synthesis of molded monolithic porous polymers using supercritical carbon dioxide as the porogenic solvent. Adv Mater 1999;11:1270–4.
[28] Wood CD, Cooper AI. Synthesis of macroporous polymer beads by suspension polymerization using supercritical carbon dioxide as a pressure adjustable porogenic solvent. Macromolecules 2001; 34:5–8.
[29] Kendall JL, Canelas DA, Young JL, DeSimone JM. Polymerizations in supercritical carbon dioxide. Chem Rev 1999;99:543–63.
[30] Cooper AI. Polymer synthesis and processing using supercritical carbon dioxide. J Mater Chem 2000;10:207–34.
[31] Cooper AI. Recent developments in materials synthesis and processing using supercritical CO_2. Adv Mater 2001;13:1111–4.
[32] Jessop PG, Leitner W. Chemical synthesis using supercritical fluids. Weinheim: Wiley, VCH; 1999.
[33] Loy DA, Russick EM, Yamanaka SA, Baugher BM, Shea KJ. Direct formation of aerogels by sol-gel polymerizations of alkoxysilanes in supercritical carbon dioxide. Chem Mater 1997; 9:2264–8.
[34] Parks KL, Beckman EJ. Generation of microcellular polyurethane foams v a polymerization in carbon dioxide. 1. Phase behavior of polyurethane precursors. Polym Eng Sci 1996;36: 2404–16.
[35] Parks KL, Beckman EJ. Generation of microcellular polyurethane foams v a polymerization in carbon dioxide. 2. Foam formation and characterization. Polym Eng Sci 1996;36:2417–31.
[36] Shi C, Huang Z, Kilic S, Xu J, Enick RM, Beckman EJ, Carr AJ, Melendez RE, Hamilton AD. The gelation of CO_2: a sustainable route to the creation of microcellular materials. Science 1999;286: 1540–3.
[37] Howdle SM, Watson MS, Whitaker MJ, Popov VK, Davies MC, Mandel FS, et al. Supercritical fluid mixing: preparation of thermally sensitive polymer composites containing bioactive materials. Chem Commun 2001:109–10.
[38] Butler R, Davies CM, Cooper AI. Emulsion templating using high internal phase supercritical fluid emulsions. Adv Mater 2001;13:1459–63.
[39] Cooper AI, Hems WP, Holmes AB. Synthesis of cross-linked polymer microspheres in supercritical carbon dioxide. Macromol Rapid Commun 1998;19:353–7.
[40] Cooper AI, Hems WP, Holmes AB. Synthesis of highly cross-linked polymers in supercritical CO_2 by heterogeneous polymerization. Macromolecules 1999;32:2156–66.
[41] Hebb AK, Senoo K, Bhat R, Cooper AI. Structural control in porous cross-linked poly (methyacrylate) monoliths using supercritical carbon dioxide as a 'pressure-adjustable' porogenic solvent. Chem Mater 2003;15:2061–69.
[42] Perrut M. Supercritical fluid applications: industrial developments and economic issues. Ind Eng Chem Res 2000;39:4531–5.
[43] McCulloch A. CFC and Halon replacements in the environment. J Fluorine Chem 1999;100:163–73.
[44] Blondino FE, Byron PR. Surfactant dissolution and water solubilization in chlorine-free liquified gas propellants. Drug Dev Ind Pharm 1998;24:935–45.
[45] Abbott AP, Eardley CA, Harper JC, Hope EG. Electrochemical investigations in liquid and supercritical 1,1,1,2-tetrafluoroethane (HFC 134a) and difluoromethane (HFC 32). J Electroanal Chem 1998;457:1–4.
[46] Abbott AP, Eardley CA. Electrochemical reduction of CO_2 in a mixed supercritical fluid. J Phys Chem B 2000;104:775–9.
[47] Tan CS, Lin HY. Precipitation of polystyrene by spraying polystyrene-toluene solution into compressed HFC-134a. Ind Eng Chem Res 1999;38:3898–902.
[48] Tan CS, Chang WW. Precipitation of polystyrene from toluene with HFC-134a by the GAS process. Ind Eng Chem Res 1998;37: 1821–6.
[49] Catchpole OJ, Proells K. Solubility of squalene, oleic acid, soya oil, and deep sea shark liver oil in subcritical R134a from 303 to 353 K. Ind Eng Chem Res 2001;40:965–72.
[50] Utracki LA, Simha R. Free volume and viscosity of polymer-compressed gas mixtures during extrusion foaming. J Polym Sci B, Polym Phys 2001;39:342–62.
[51] Wood CD, Senoo K, Martin C, Cuellar J, Cooper AI. Polymer synthesis using hydrofluorocarbon solvents. 1 Synthesis of cross-linked polymers by dispersion polymerization in 1,1,1,2-tetrafluoroethane Macromolecules 2002;35:6743–6.
[52] Wood CD, Cooper AI. unpublished results.
[53] Dinoia TP, Conway SE, Lim JS, McHugh MA. Solubility of vinylidene fluoride polymers in supercritical CO_2 and halogenated solvents. J Polym Sci B, Polym Phys 2000;38:2832–40.
[54] Defibaugh DR, Moldover MR. Compressed and saturated liquid densities for 18 halogenated organic compounds. J Chem Eng Data 1997;42:160–8.